2018 25th International Lightning Detection Conference &
7th International Lightning Meteorology Conference
March 12 - 15 | Ft. Lauderdale, Florida, USA

Monthly GLD360 Lightning Percentages by Continent

Ronald L. Holle[1]
Ryan K. Said[2]
William A. Brooks[1]
[1]Vaisala Inc., Tucson, Arizona, USA
[2]Vaisala Inc., Louisville, Colorado, USA
ron.holle@vaisala.com

***Abstract*—Continuous detection by Vaisala's Global Lightning Dataset GLD360 network now makes it possible to examine lightning across the globe. This study apportions continent-scale detection of 8.8 billion strokes from 2013 through 2017 by month through the year. Northern Hemisphere lightning peaks from May through September, while Southern Hemisphere strokes peak from November through March. North America, Europe, and Asia have a concentration of lightning in summer, although the annual distribution for Asia is not as distinct since part of the continent extends to the equator. South America and Australia have peak lightning from November through February. Africa shows only minor monthly variations throughout the year since the regions north of the equator have more lightning in the Northern Hemisphere summer, and the reverse in the south. These observations, along with complementary human casualty research, allow for a better understanding of lightning impacts on life and property around the world.**

Keywords—Lightning, continents, GLD360, annual variations

I. Introduction

Continuous global lightning detection is now possible with the use of advanced technology that was not previously available. Better documentation of the occurrence of lightning can provide a cohesive view of where and when lightning occurs on the broad scale for identifying and planning for the effects of lightning on people [Roeder et al., 2015; Holle, 2016] and infrastructure, as well as studies of geophysical properties. Comparisons will be made of lightning occurrence over a broad scale by continent, hemisphere and land-ocean comparisons by examination of monthly variations through the year.

Vaisala's Global Lightning Dataset (GLD360) underwent a major algorithm upgrade in 2015 that improved the detection capability of this lightning locating system around the world. The algorithms have been applied retroactively to historical data starting on 01 January 2012. In this present study, data from the latest five years of 2013 through 2017 are used, totaling 8.8 billion strokes over all oceans and continents. Holle et al. [2017] showed similar analyses with data from 2012 through 2016. A lightning flash has several individual discharges within them called strokes. GLD360 detections are primarily individual cloud-to-ground (CG) strokes, while the remainder are the typically weaker in-cloud (IC) pulses than CG strokes. Individual classification of which detection is CG versus IC is an active Vaisala research topic. The continuous detection of the location and time of two billion lightning events each year has resulted in an unprecedented opportunity to improve the broad-scale view of lightning occurrence [Poelman et al., 2013; Pohjola and Mäkelä, 2013; Said et al., 2013; Mallick et al., 2014; Said and Murphy, 2016].

II. Global Lightning Detection

Real-time, continuous and relatively uniform detection of much of the lightning over the entire globe was not readily available until Vaisala's GLD360 network was established. Especially important is the detection over less-populated landmasses and the oceans far from land. No single satellite continuously monitors all areas of the world, and other ground-based networks require numerous sensors with moderately short distances between them, such that remote land and ocean areas are often poorly covered. In contrast, GLD360 uses both time-of-arrival and magnetic direction-finding techniques at each sensor, with other attributes to allow geo-location of lightning strokes at distances up to 7,000 km from each sensor.

Specific features of radio atmospherics that are generated by lightning discharges are detected by GLD360 in the very low frequency range through the use of a waveform recognition algorithm. A propagation correction is applied to account for the time delay of each waveform feature as it arrives at each sensor. Due to attenuation with distance, a model is also applied to the amplitude of the waveform to recover an estimate of the peak current.

An updated location algorithm was released by Vaisala on 18 August 2015 that doubled the number of detections in the GLD360 dataset [Said and Murphy, 2016]. The primary algorithm changes were a more refined propagation model, improved sensor correlation heuristics, and a more robust backend infrastructure. All data since 01 January 2012 were reprocessed with the upgraded detection algorithm. The resulting map in Fig. 1 shows the dataset for the latest five years from 2013 through 2017, comprised of 8,761,390,744 strokes. It is apparent that lightning occurs predominantly over land, and oceanic lightning tends to be located near the continents rather than far from land.

While the long-range GLD360 network detects the majority of global CG flashes, the detection of weaker CG and IC lightning is relatively non-uniform. A proper calibration of the absolute flash detection efficiency that corrects for this variability is beyond the scope of this paper. Dividing the monthly stroke counts by the total for each region effectively calibrates the results against spatial variations in detection efficiency and the IC:CG ratio. This normalization scheme does not, however, calibrate against temporal variations. Infrastructure improvements and temporal fluctuations in sensor availability (usually due to power and communication outages) affect the distribution of counts. The five-year time average and month-long count bins should partially mitigate this remaining variability.

The following analyses will address hemispheric, land-ocean, and continental-scale features by month of the year that are based on the data in Fig. 1. The spatial definition of the continents used in this study is shown in Fig. 2 where the equator is also indicated.

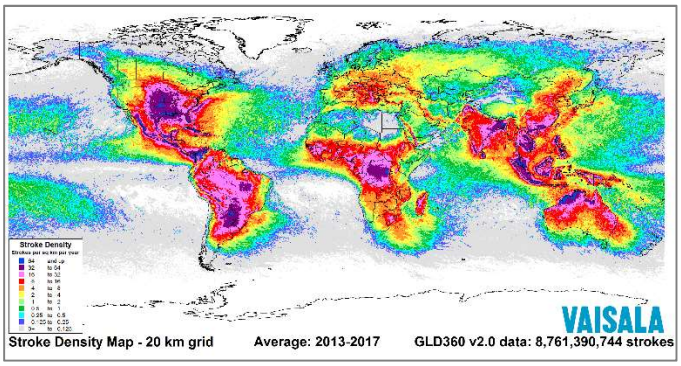

Fig. 1. Lightning stroke density per square km per year from GLD360 for the globe from 2013 through 2017. The density map depicts a total of 8,761,390,744 strokes. Scale is at lower left; grid size is 20 by 20 km.

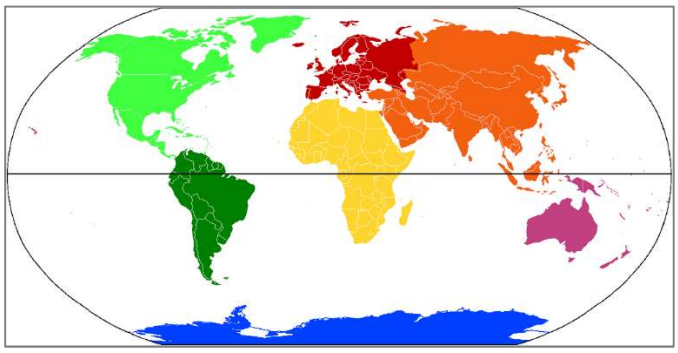

Fig. 2. Color depiction of continents used in this study; black line indicates equator.

III. Hemispheric and Land-ocean Comparisons

The first comparison is between hemispheres, as shown in Fig. 3. The scale is the percentage of the yearly lightning detected within each hemisphere by month. There is a distinct lightning maximum in the Northern Hemisphere in the summer months of May through September, while the Southern Hemisphere has the most lightning in its summer months of November through March. Both hemispheres have quite small values during their respective winters.

The annual curves for all of the world's landmasses compared with all oceans show that the monthly differences between land and water are small (Fig. 4). The largest amounts of lightning for both areas are in the May through September period (Fig. 4). Fig. 1 indicates that a large amount of oceanic lightning occurs near land, and is associated with thunderstorms that occurred and/or initiated over land. Since there is more land in the Northern Hemisphere, that hemisphere also dominates the annual oceanic cycle.

IV. Monthly Changes by Continent

How lightning varies through the year by continent is shown in Fig. 5. Continents in the Northern Hemisphere have a lightning maximum centered on the month of July and small amounts of lightning in their winter months. The opposite occurs in Southern Hemisphere continents. Africa, however, is uniform throughout the year due to its location on both sides of the equator, so its annual variations north and south of the equator are separated in Fig. 6.

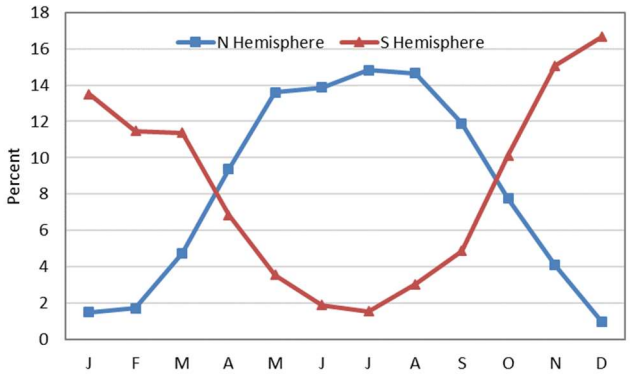

Fig. 3. Lightning stroke percentages by month for the Northern and Southern Hemispheres.

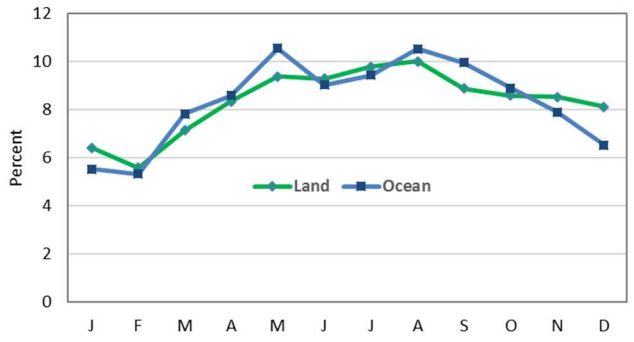

Fig. 4. Lightning stroke percentages by month over all land and ocean areas of the world.

The annual variation of lightning over each continental landmass in Fig. 5 indicates the following features:

- **North America:** Small percentages of lightning occur after the first of the year. A steady increase in lightning to a July maximum is followed by a more rapid decline, as was also documented for the United States [Holle et al., 2016].
- **South America:** The annual cycle is opposite to that of the Northern Hemisphere. Lightning is most frequent during the summer months starting in October, and is at a minimum during June and July when drier cooler air prevails over all but the Amazon region. A maximum in lightning lasting through most of the year has been identified over northern South America by Albrecht et al. [2016] and Holle and Murphy [2017].
- **Europe:** The summer maximum is very strong and the winter minimum is very weak. However, note in Fig. 1 that Europe has much less lightning than North America. Numerous regional and national climatologies using ground-based detection networks have been performed over Europe such as those by Anderson and Klugmann [2014] and Marcos-Menéndez et al. [2016].
- **Africa:** The continent's annual cycle is very weak in Fig. 5, primarily because the continent's equatorial regions have lightning all year long [Albrecht et al., 2016]. Fig. 6 indicates that the Northern Hemisphere summer affects regions north of the equator to result in frequent lightning during those months. Frequent lightning in the area of Africa south of the equator occurs during the Southern Hemisphere summer (Fig. 6). The result is close to a constant distribution through the year as shown in Fig. 5. The only African climatologies using ground-based lightning detection networks have been compiled over South Africa [Gijben, 2012] and Malawi [Kalindekafe et al., 2018].
- **Asia:** Most of the continent is located north of the equator (Fig. 2). The result is a broad maximum of strokes from May through August. However, there are very active lightning areas near the equator (Fig. 1) that contribute strokes all year. As a result, Northern Hemisphere winter months have higher lightning percentages than in North America and Europe. Among the many ground-based lightning detection climatologies for Asia is that of Sugita and Matsui [2014].
- **Australia:** The continent is located entirely south of the equator and has the best-defined Southern Hemisphere pattern. A distinct maximum in monthly stroke percentages occurs around the first of the year and a near-zero minimum is in winter.
- **Antarctica:** There is no detected lightning, although extensions of thunderstorms formed over South America extend toward the South Shetland Islands (Fig. 1).

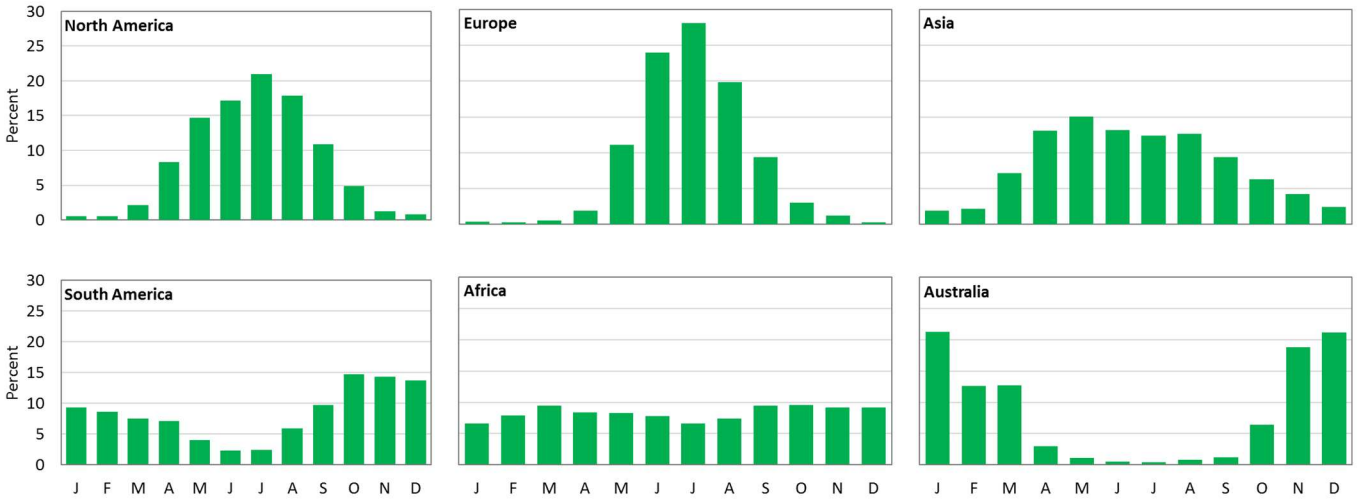

Fig. 5. Lightning stroke percentages by month for each continent.

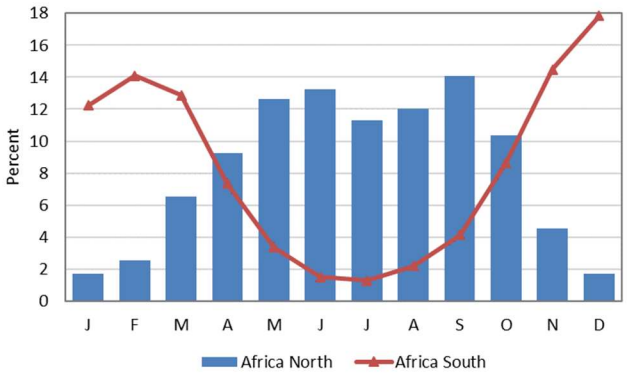

Fig. 6. Lightning stroke percentages by month in Africa north and south of the equator.

V. SUMMARY

The development of spatially and temporally continuous lightning detection around the world by Vaisala's GLD360 makes it possible to examine broad categories of occurrence. Five years of 8,761,390,744 strokes from 2013 through 2017 were apportioned through the year by month. Opposite annual cycles in detected lightning are identifiable between the two hemispheres. The annual variation over global oceans is similar to that over land in the Northern Hemisphere because storms move offshore from those continents more often than the smaller Southern Hemisphere land areas. The summer months of May through September have the most lightning in North America, Europe, and Asia. November through February are the months with the most lightning in South America and Australia. Over Africa, the annual cycle for the year is nearly uniform, but lightning north of the equator is aligned with the Northern Hemisphere summer, and the reverse applies to the south of the equator. These global observations, when combined with national and regional lightning climatologies and human casualty summaries, can be expected to improve understanding of the impacts of lightning on life and property.

REFERENCES

Albrecht, R. I., S. J. Goodman, D. E. Buechler, R. J. Blakeslee, and H. J. Christian (2016), Where are the lightning hotspots on Earth?, Bull. Amer. Meteor. Soc., 97, 2051–2068.

Anderson, G., and D. Klugmann (2014), A European lightning density analysis using 5 years of ATDnet data, Nat. Hazards Earth System Sci., 14, 815-829.

Gijben, M. (2012), The lightning climatology of South Africa, S. African J. Sci., 108, Article 740, doi:10.4102/sajs.v108i3/4.740.

Holle, R. L. (2016), A summary of recent national-scale lightning fatality studies, Weather, Climate, and Society, 8, 35-42.

Holle, R. L., and M. J. Murphy (2017), Lightning over three tropical lakes and the Strait of Malacca: Exploratory analyses, Mon. Wea. Rev., 145, 4559-4573.

Holle, R. L., K. L. Cummins, and W. A. Brooks (2016), Seasonal, monthly, and weekly distributions of NLDN and GLD360 cloud-to-ground lightning, Mon. Wea. Rev., 144, 2855-2870.

Holle, R. L., R. Said, and M. Scott (2017), Global lightning variations: Lightning for each continent through the year, Met. Tech. Intl., 1039-1240.

Kalindekafe, L., R. L. Holle, S. Gondwe, V. Katonda, and M. Mkandawire (2018), Spatial and temporal distributions of Malawi lightning in January 2017, paper presented at the 25th International Lightning Detection Conference, Vaisala, Fort Lauderdale, Florida, 9 pp.

Mallick, S., V. A. Rakov, T. Ngin, W. R. Gamerota, J. T. Pilkey, J. D. Hill, M. A. Uman, D. M. Jordan, A. Nag, and R. K. Said (2014), Evaluation of the GLD360 performance characteristics using rocket-and-wire triggered lightning data, Geophys. Res. Lett., 41, 3636–3642.

Marcos-Menéndez, J. L., F. Castedo-Dorado, and J. R. Rodríguez-Pérez (2016), Statistical characterization of cloud-to-ground lightning data and meteorological modelling of cloud-to-ground lightning days for the warm season in the province of León (northwest Spain), Meteor. Appl., 23, 671-682.

Poelman, D. R., W. Schulz, and C. Vergeiner (2013), Performance characteristics of distinct lightning detection networks covering Belgium, J. Atmos. Oceanic Technol., 30, 942–951.

Pohjola, H., and A. Mäkelä (2013), The comparison of GLD360 and EUCLID lightning location systems in Europe, Atmos. Res., 123, 117–128.

Roeder, W. P., B. H. Cummins, K. L. Cummins, R. L. Holle, and W. S. Ashley (2015), Lightning fatality risk map of the contiguous United States, Natural Hazards, 79, 1681-1692.

Said, R., and M. J. Murphy (2016), GLD360 upgrade: Performance analysis and applications, paper presented at the 24th International Lightning Detection Conference, Vaisala, San Diego, Calif., 8 pp.

Said, R., M. B. Cohen, and U. S. Inan (2013), Highly intense lightning over the oceans: Estimated peak currents from global GLD360 observations, J. Geophys. Res. Atmos., 118, 6905–6915.

Sugita, A., and M. Matsui (2014), The frequency of lightning activity in Hokkaido as observed by the JLDN from 2000 to the present, paper presented at the 5th International Lightning Meteorology Conference, Vaisala, Tucson, 4 pp.